Constructing random matrices to represent real ecosystems

Alex James[1] Michael J. Plank[2] Axel G. Rossberg[3]

Jonathan Beecham[4] Mark Emmerson[5] Jonathan W. Pitchford[6]

1. Corresponding author. alex.james@canterbury.ac.nz.
Biomathematics Research Centre, University of Canterbury, New Zealand.
Te Pūnaha Matatini, New Zealand.

2. michael.plank@canterbury.ac.nz.
Biomathematics Research Centre, University of Canterbury, New Zealand.
Te Pūnaha Matatini, New Zealand.

3. Axel@rossberg.net.
Centre for Environment, Fisheries and Aquaculture Science (Cefas), Lowestoft, UK
School of Biological Sciences, Queens University Belfast, UK.

4. jonathan.beecham@cefas.co.uk.
Centre for Environment, Fisheries and Aquaculture Science (Cefas), Lowestoft, UK.

5. m.emmerson@qub.ac.uk.
School of Biological Sciences, Queens University Belfast, UK.

6. jon.pitchford@york.ac.uk.
Departments of Biology and Mathematics, University of York, UK.

Keywords: community matrix; complexity; food web; interaction strength; stability; predator–prey interaction.

Online version also includes Appendices.

Article type: Article

Abstract

Models of complex systems with n components typically have order n^2 parameters because each component can potentially interact with every other. When it is impractical to measure these parameters, one may choose random parameter values and study the emergent statistical properties at the system level. Many influential results in theoretical ecology have been derived from two key assumptions: that species interact with random partners at random intensities and that intraspecific competition is comparable between species. Under these assumptions, community dynamics can be described by a community matrix which is often amenable to mathematical analysis. We combine empirical data with mathematical theory to show that both these assumptions lead to results that must be interpreted with caution.

We examine 21 empirically derived community matrices constructed using three established, independent methods. The empirically derived systems are more stable by orders of magnitude than results from random matrices. This consistent disparity is not explained by existing results on predator–prey interactions. We investigate the key properties of empirical community matrices that distinguish them from random matrices. We show that network topology is less important than the relationship between a species' trophic position within the food web and its interaction strengths. We identify key features of empirical networks that must be preserved if random matrix models are to capture the features of real ecosystems.

1 Introduction

Interactions between species are central to the concept of an ecosystem. They are, however, both expensive and technically challenging to measure empirically. It is natural, therefore, that ecologists have sought to understand to what extent these interactions can be thought of as random, and furthermore to understand and quantify the possible relationships between these interactions which best confer the features of ecosystem stability, resilience and dynamics observed in nature. For these reasons, theories involving randomly generated interactions between species have underpinned many influential ideas concerning the stability of complex ecological networks (May, 1972; Pimm and Lawton, 1978; Yodzis, 1981; Bastolla et al., 2009; Allesina and Tang, 2012).

May (1972) famously showed that, under certain assumptions, there is a limit on how "complex" a network ecosystem with a stable equilibrium can be. He then hypothesized that this was relevant to the stability of ecological networks. Stability, in this context, means there is an equilibrium in which all species in the network survive at some positive density, and that this equilibrium is robust to sufficiently small perturbations in the species densities. Under this definition, stability of the equilibrium is quantified by the leading eigenvalue of the Jacobian matrix evaluated at the equilibrium point, which describes the behaviour of the system close to equilibrium. Whether complex ecosystems operate close to equilibrium is matter of some debate, and local stability is not the only way of quantifying the resilience of an ecosystem to change (Grimm and Wissel, 1997; McCann, 2000). Other measures include, for example, permanence (Jansen, 1987; Law and Blackford, 1992), persistence (Bastolla et al., 2009; Thébault and Fontaine, 2010; Gravel et al., 2011) and species-deletion stability (Pimm, 1980). Nevertheless, local stability is a necessary condition for a persistent equilibrium and is a widely used measure of ecosystem robustness (Thébault and Fontaine, 2010; Allesina and Tang, 2012; Staniczenko et al., 2013) and we focus on local stability in this paper.

The conclusions of May (1972) contradicted earlier ideas that ecosystems with more species, and more interactions among those species, are more likely to be stable (MacArthur, 1955; Elton, 1958). In reality, highly complex ecological networks, i.e. networks with many species, many interactions and strong interactions, do exist (O'Gorman and Emmerson, 2010; Twomey et al., 2012) and empirical evidence frequently points to a positive relationship between complexity and stability (Yodzis, 1981; De Ruiter et al., 1995; McCann, 2000; Gravel et al., 2011). Various theoretical explanations for this apparent "stability despite complexity" have been proposed, including a skew in the interaction strength distribution towards weak links (McCann et al., 1998; Emmerson and Yearsley, 2004), weak links in long loops (Neutel et al., 2002), a pyramidal distribution of biomass across trophic levels (Neutel et al., 2007), the stabilising effect of predator–prey interactions (De Angelis, 1975; Allesina and Pascual, 2008) and spatial colonization–extinction dynamics (Gravel et al., 2011). Interaction strengths are widely accepted to be very important, but the consequences for theoretical structure–stability relationships are not well understood.

Our aim is to explore the relative importance of some of these hypotheses for stability despite complexity, and to investigate the consequences of two key assumptions we identify in random matrix models. To do this, we use 21 networks constructed from empirical data via three independent methods. A combination of numerical simulations, statistical analysis and algebraic calculations is used to assess the important features of these empirically derived networks within the wider class of random models which aim to describe them.

The first assumption of May (1972) concerns the interactions between species. Species were assumed to interact with one another randomly, so that the architecture of the network, i.e. which elements of the community matrix are non-zero, was described by an Erdős–Rényi random graph (Erdős and Rényi, 1960). The strengths assigned to species interactions, i.e. the weights of the non-zero network links, were normally distributed.

To test the assumption of randomly generated interactions and intensities, we quantify the stability of the empirically derived food webs and compare this to the stability predicted by a random matrix. We use a suite of randomization algorithms with different assumptions about food web structure and interaction strength distributions. In almost all cases, we find that each empirically derived food web is substantially more stable than the corresponding randomized food webs. This shows that the assumptions built into the random matrices bias the results towards instability.

The second assumption concerns the intraspecific competition of each species. May (1972) assumed that all species had the same timescale for self-regulation at equilibrium, resulting in equal elements on the diagonal of the community matrix. We use simple dynamical systems analysis to show that normalising the self-regulation terms in this way leads to a model that is not representative of real communities. In ecological terms, this requires a highly restrictive and untested assumption about trade-offs between species' intrinsic growth rates and their interactions with other species. We investigate the consequences of this assumption by exploring the effect on matrix stability of different methods for estimating the self-regulation terms. In contrast to the "random interactions" assumption above, the consequence of assuming equal self-regulation is a strong bias towards stability.

2 Random matrix models

We assume that a given ecosystem comprises n species, and that the population of each species is represented by its biomass density x_i, where $i = 1, ..., n$. The dynamics of the system are then represented by a general system of differential equations,

$$\frac{d\mathbf{x}}{dt} = \mathbf{f}(\mathbf{x}), \tag{1}$$

where $\mathbf{x} = (x_1, ..., x_n)$ and $\mathbf{f}$ is a function which depends on $\mathbf{x}$. We define the Jacobian matrix in its mathematical sense to mean the matrix describing the linearised dynamics at any given location (Wiggins, 2003) i.e.

$$J_{ij} = \frac{\partial f_i}{\partial x_j}. \tag{2}$$

When this matrix is evaluated at an equilibrium point of the system, i.e. at a point $\mathbf{x}^*$ such that $\mathbf{f}(\mathbf{x}^*) = \mathbf{0}$, it is referred to as a community matrix. This is closely related to, but distinct from, the matrix of coefficients of species interaction rates used to parameterise, for example, a Lotka–Volterra model (see Sec. 4). Local stability of an equilibrium is determined by the real part of the leading eigenvalue (i.e. eigenvalue with largest real part) of its associated community matrix: if that real part is negative then the equilibrium is locally stable. Although stability is a binary on/off property, for stable equilibria we use the term "less stable" to mean "further from stability" (i.e. having a leading eigenvalue with larger real part), and conversely for "more stable".

May (1972) modelled ecological networks of S species using random $S \times S$ community matrices, A. Each off-diagonal element a_{ij} of A is set to zero with probability $1 - C$ and drawn from a distribution with mean zero and variance σ^2 with probability C. The element a_{ij} represents the effect of a unit of species j on the rate of increase of species i at equilibrium: if a_{ij} is zero, species j has no direct effect on species i. The parameter C is referred to as the connectance. May's critical insight was to use Wigner's semicircle theorem and the circular law of Metha (1967) to show that the real parts of the eigenvalues of this random matrix must all be less than

$$d_0 = \sigma\sqrt{SC}. \tag{3}$$

The variable d_0 is commonly referred to as "complexity" and represents the relative strength of intraspecific competition needed to stabilise a given food web. If the diagonal

elements a_{ii}, representing the effects of intraspecific competition, are all set to $-d_0$, then all the eigenvalues of the community matrix will have negative real parts and the equilibrium will be stable (see Sec. 4). A matrix with a high value of d_0 requires strong intraspecific competition to stabilise it. May (1972) used Eq. (3) to conclude that high connectance (large C), a large number of species (large S) or strong interactions (high σ) in food webs leads to instability.

These results were generalised by Allesina and Tang (2012) to community matrices with a more specific structure in the interaction terms a_{ij}. This included predator–prey systems in which interactions are beneficial to one species and detrimental to the other (a_{ij} and a_{ji} have opposite signs). Tang et al. (2014) extended the stability condition to account for pairwise correlation between a_{ij} and a_{ji}. They showed that, with high probability, the leading eigenvalue of the community matrix will have real part less than

$$d_0 = \sqrt{SV}(1 + \rho) - E, \tag{4}$$

where ρ is the correlation between a_{ij} and a_{ji} and E and V are the mean and variance of the off-diagonal elements (including zeros). This result, with its revised definition of complexity, indicates that (under the assumptions of random network topology) the negative pairwise correlation ($\rho < 0$) one might expect to find in a predator–prey system should be a stabilising factor.

3 The relationship between random matrices and real food webs

There are numerous methods of constructing a community matrix from data, many of which rely on body-size data, allometric scaling relationships, bio-energetic models and/or interaction strength data. Brose et al. (2006), Otto et al. (2007) and Woodward et al.

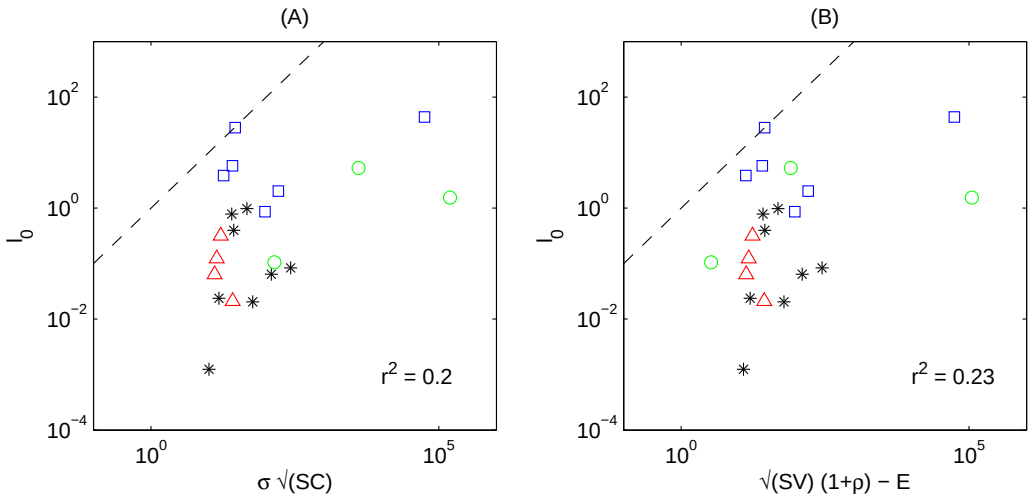

Figure 1: **The stability–complexity relationship in 21 empirically derived food webs.** The real part l_0 of the leading eigenvalue against complexity d_0 defined by: (A) Eq. (3); (B) Eq. (4). S is the number of species, C is the connectance, σ^2 is the variance of non-zero off-diagonal elements, E and V are the mean and variance of all off-diagonal elements and ρ is the correlation coefficient between a_{ij} and a_{ji} pairs. Diagonal elements are set to zero. The dashed lines show the line $l_0 = d_0$. Symbols indicate the method used to construct the community matrix: biomass flux = black stars (successional webs) or red triangles (soil webs); EwE = blue squares; PPMR = green circles. Although complexity is correlated with stability, the relationship is weak and of little practical relevance. Many of the empirically derived networks are many orders of magnitude more stable than predicted by the criteria in Eq. (3) and (4).

(2005*a*) explored the consequences of some of these assumptions and highlighted their importance in determining stability. We use three independent, established approaches, each relying on different sets of assumptions, to construct community matrices from empirical data from 21 food webs with distinct topologies. These consist of: (i) eight successional food webs and four soil food webs constructed using the "biomass flux" method of Moore et al. (1996); Neutel et al. (2002); (ii) six marine ecosystems modelled using Ecopath with Ecosim (EwE) (Christensen and Pauly, 1992); (iii) three freshwater/estuarine ecosystems constructed using the predator–prey mass ratio (PPMR) model of Emmerson and Raffaelli (2004). See Appendix A for details. The soil and freshwater systems are all food webs consisting only of predator–prey interactions; the marine systems contain a mixture of interaction types.

We set the diagonal elements of each empirically derived matrix to zero and calculate the

real part l_0 of the leading eigenvalue as a measure of how far that matrix is from stability (May, 1972; Neutel et al., 2002; Allesina and Tang, 2012). Fig. 1A plots l_0 against complexity as defined by Eq. (3). Complexity is inversely correlated with stability, but only weakly, and predicts stability within two orders of magnitude at best. Fig. 1B repeats the plot using the modified stability condition incorporating pairwise correlation in Eq. (4) (Tang et al., 2014). The only matrices for which Eq. (4) provides a substantially better prediction are the food webs constructed with the PPMR model (green circles), which result in a strong negative pairwise correlation (Emmerson and Raffaelli, 2004). The construction methods used in the other networks (see Appendix A) result in much weaker pairwise correlation and accounting for it using Eq. (4) has almost no effect.

Fig. 1 raises the important question: given that complexity alone cannot usefully predict stability in these empirically derived networks, which other network properties can? We test the hypothesis that randomly generated community matrices capture the essential properties of a real food web by comparing suites of randomly generated matrices to the empirically derived matrices, where each suite is defined by a set of ecologically motivated rules. We seek algorithms capable of emulating key properties of the empirical networks.

For each empirically derived matrix, we generate suites of 200 random matrices for each of 12 randomization algorithms and calculate the value of l_0 for each randomization. If a particular network property is fundamental to stability, then alterations to the network that preserve this property should only minimally affect stability. Fig. 2 shows the results of this process for one empirically derived community matrix. Every randomized matrix has the same size and connectance as the empirically derived matrix. The red line shows the real part of the leading eigenvalue of the empirically derived matrix, $l_0 = 0.1$. The histograms show the distribution of l_0 generated by 200 realisations of each randomization algorithm.

Fig. 2A shows the distribution for the random matrix proposed by May (1972): the network topology is Erdős–Rényi; the non-zero entries are drawn from a normal distribution

with zero mean and the same variance as in the original matrix. The difference is striking: in the random matrices, the strength of intraspecific competition needed to stabilise the food web, l_0, is between 100 and $10,000$ times greater than in the original matrix. Fig. 2B shows the distribution of l_0 for a network as in A, but with the same pairwise sign structure (i.e. the same number of predator–prey and competitive interactions) as the original matrix. These interaction pairs are randomly placed in the matrix and the positive and negative elements are randomly and independently generated from half-normal distributions with the same mean as in the original matrix. This approach is similar to that of Pimm and Lawton (1978) and Allesina and Tang (2012). This randomization still gives values of l_0 approximately 100 times larger than in the original matrix. Fig. 2C uses the same algorithm as B to generate the interaction strengths, but preserves the empirical network topology rather than generating a topology at random. This is similar to an algorithm used by Jacquet et al. (2013). The difference in intraspecific interaction strength needed to stabilise the webs, l_0, between the randomizations and the empirically derived matrix is still large.

The preceding randomization algorithms all randomly generate non-zero elements of the community matrix from normal distributions and give values of l_0 that are consistently more than 100 times greater than in the original matrix. Given this failure of randomly generated elements to capture the properties of the empirically derived matrices, we test a second category of algorithms that permute the actual matrix elements, rather than randomly generating new elements. Fig. 2E shows the distribution of l_0 from an algorithm which moves existing pairs of interactions, i.e. which destroys the topology of the original network, but holds (a_{ij}, a_{ji}) pairs together and preserves pairwise correlation ρ. This algorithm gives a marked improvement over Fig. 2A–C in retaining the original matrix properties: for this network, the value of l_0 for the empirically derived matrix is now within the interquartile range of the distribution of l_0 under the randomization. In Fig. 2F, pairs of elements (a_{ij}, a_{ji}) are swapped with other existing pairs of elements, thus preserving the topology of the network. This additional constraint does very little

to bring the stability of randomized matrices closer to that of the empirically derived matrices on which they are based. Finally, Fig. 2G applies a permutation of the positive elements and an independent permutation of the negative elements. This preserves the original topology and sign structure, but destroys any pairwise correlation. Again, this modification gives very little change relative to algorithms E and F. Algorithms F and G are similar to those used by Yodzis (1981); De Ruiter et al. (1995); Neutel et al. (2002).

Algorithms E–G, which use the original matrix elements rather than replacing them with random numbers, show a marked improvement in preserving the stability of the original matrix. This shows that the methods used to estimate the community matrices produce off-diagonal elements that yield relatively stable communities, even if these elements are permuted and the topological structure of the original empirical networks is destroyed. The observation that there is little difference between E, F and G shows that network topology (preserved in F and G) and pairwise correlation (preserved in E and F) are less important, in this particular community, than the distribution of matrix elements.

We repeated the above analysis using all 21 empirically derived community matrices (see Appendix A). We define the error for a random matrix to be $\log_{10}(l_{\mathrm{rand}}/l_{\mathrm{emp}})$, where l_{rand} and l_{emp} are the values of l_0 in the randomized and empirically derived matrix respectively. Fig. 3 shows the mean and the 5^{th} to 95^{th} percentile range of the error for each randomization algorithm, applied to each of the 21 food webs. When these intervals exclude zero, the value of l_0 for the empirically derived matrix lies in the tail of the distribution of l_0 under the randomization scheme, showing that the scheme does not capture the relevant properties of the original matrix. The results in Fig. 3 confirm that the patterns seen in Fig. 2 for a single successional soil food web extend across a range of food webs. For the randomization algorithms that use normally distributed elements (A–C), the predictions are particularly biased, showing that the random matrices are much further from stability than the empirically derived matrices. The distributions of l_0 for these algorithms are relatively narrow, showing the similarity of all matrices generated by

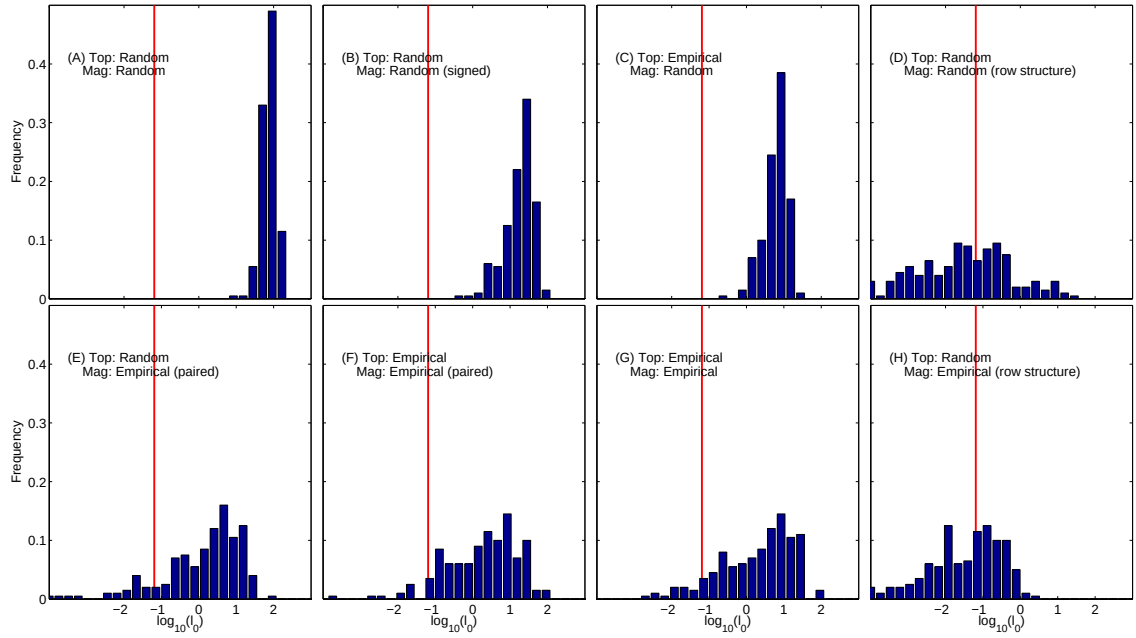

Figure 2: **Randomized matrices are statistically many orders of magnitude less stable than the empirically derived matrix on which they are based.** Graphs show the distribution of the strength of intraspecific competition needed to stabilise the web, l_0 (the real part of the leading eigenvalue), for six different randomization algorithms, changing either or both of network topology (Top) and magnitude of interaction strengths (Mag), applied to an empirically derived community matrix (a successional soil food web). The red line shows the value of l_0 for the empirically derived matrix. Randomizations that use a normal distribution to generate the non-zero elements (A–C) are orders of magnitude less stable than the empirically derived matrices; randomizations that move or swap the actual matrix elements (E–G) are closer, but still show a consistent bias towards instability; randomizations that preserve row structure (D and H) better reflect the stability of the empirically derived matrices. See Appendix B for details of the randomization algorithms.

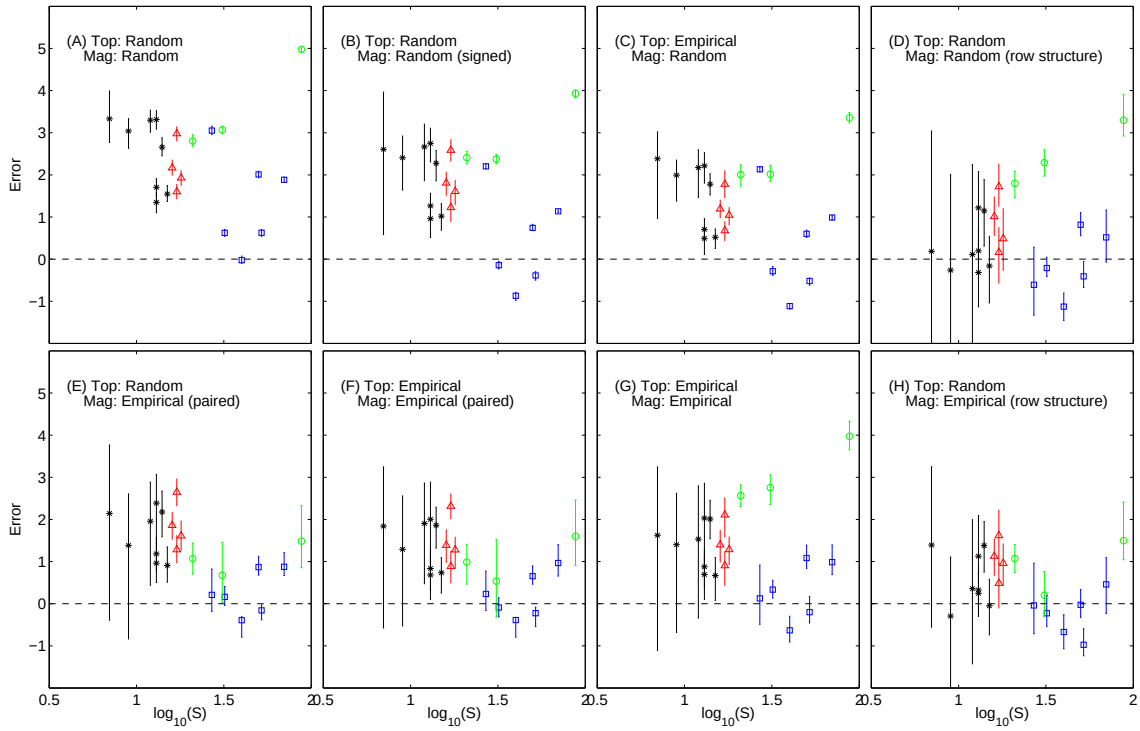

Figure 3: **Differences in stability between empirically derived and randomized matrices across 21 communities and three construction methods.** The distribution of error = $\log_{10}(l_{\text{rand}}/l_{\text{emp}})$ for the same six randomization algorithms (A–H) as in Fig. 2, changing either or both of network topology (Top) and magnitude of interaction strengths (Mag). The food webs are plotted against the number of species S in the web on the horizontal axis. See Appendix B for details of the randomization algorithms. Symbols indicate the method used to construct the community matrix: biomass flux = black stars (successional webs) or red triangles (soil webs); EwE = blue squares; PPMR = green circles.

these algorithms. Importantly, all the randomization algorithms tested are consistently biased towards instability (error > 0) for the majority of matrices.

As seen in Fig 2, using the same distribution of elements (Fig. 3E–G) as in the empirically derived matrix helps to stabilise the randomized networks. Preserving either the empirical network topology (Fig. 3F, G) or pairwise correlation (Fig. 3E, F) does not further improve the results for most networks. The notable exceptions to this are the food webs constructed with the PPMR model (green circles), which have strong pairwise correlation and therefore respond well to algorithms that preserve this feature. This is consistent with the results of Tang et al. (2014), which also used PPMR in the construction methods.

The structure of predator–prey networks has been found to play an important role in stability (Levins, 1979; Dambacher et al., 2003; Allesina and Tang, 2012). A pyramidal biomass pattern leads to strong row structure in community matrices: the variance of elements within a row is much less than the variance of elements between rows (Jacquet et al., 2013). This is borne out by the definition of an element of the community matrix: a_{ij} is the effect of a unit of species j on the rate of increase of species i at equilibrium. The rate of increase of species i is typically proportional to its abundance (see Sec. 4), meaning that the magnitude of elements in row i of the community matrix should be strongly correlated with the equilibrium abundance of species i.

To test the role of row structure, we designed an algorithm that preserves the average magnitude of the elements in each row of the matrix. The positive/negative elements in each row are generated from normal distributions with the same means as in the original matrix (Figs. 2D, 3D). To investigate the role of interaction strength distribution in tandem with row structure, we designed a second algorithm that moves elements of the original matrix within rows in the lower triangle and moves the corresponding elements within columns in the upper triangle, holding pairs of elements (a_{ij}, a_{ji}) together (Figs. 2H, 3H) (see Appendix B for details). Both these algorithms destroy the original network topology, but preserve stability remarkably well in most food webs. Using randomly generated elements (Fig. 3D) destabilises community matrices constructed using the PPMR model (green circles), because it destroys the strong pairwise correlation in these matrices; the algorithm that preserves pairwise correlation (Fig. 3H) preserves stability much better for these matrices. For the other food webs, there is little difference between Figs. 3D and H, indicating that the row structure itself is more important than the precise distribution of interaction strengths.

Cycles of length three (interaction chains from species i to species j to species k and back to species i), which typically arise from omnivorous interactions in food webs, can also affect stability. Neutel et al. (2002) showed that strong top-down effects in omnivorous

relations tend to be spread across different cycles, meaning that the maximum cycle weight (where cycle weight is defined as the geometric mean of the strengths of the interactions in the cycle) tends to be lower in a real food web than in a randomized community matrix. Since cycle weights are closely linked to eigenvalues (Hofbauer and Sigmund, 1998), they proposed that this helps make food webs stable. To test the role of cycles of in our empirically derived matrices, we designed simple algorithms that only change links that are not in a cycle of length three, either destroying or preserving the original network topology. Both algorithms preserve the number of cycles of length three, their weights and the pairwise correlation of elements (see Appendix B for details). These are severe constraints: in most networks, only 25% to 35% of links are changed by these algorithms. To enable a fair comparison with randomization algorithms that do not preserve cycles of length three, we devised corresponding algorithms that change the same number of links as the cycle-preserving algorithms, but choose the links at random rather than because of their involvement in a cycle of length three. For the topology-changing algorithm (Fig. 4A), there is little difference in the mean error between the algorithm that preserves cycles of length three and the algorithm that does not. For the topology-preserving algorithm (Fig. 4B), preserving cycles of length three reduces error (see Supplementary Fig. S2 for the error distributions for each algorithm). This shows that stability is promoted by the way in which cycles are positioned within the overall network topology (which is only preserved in Fig. 4B), rather than simply by their weights (which are preserved in both Fig. 4A and B).

Of the randomization algorithms investigated, the cycle-preserving, topology-preserving algorithm (Fig. 4B) is least biased, but is highly restrictive, requiring information about the network topology, cycle structure and distribution of matrix elements. In contrast, the algorithm shown in Fig. 3D only requires the means of the community matrix elements for each species and has purely random topology. This corresponds to May-type assumptions combined with realistic sign structure (Allesina and Tang, 2012) and equilibrium biomasses for each species.

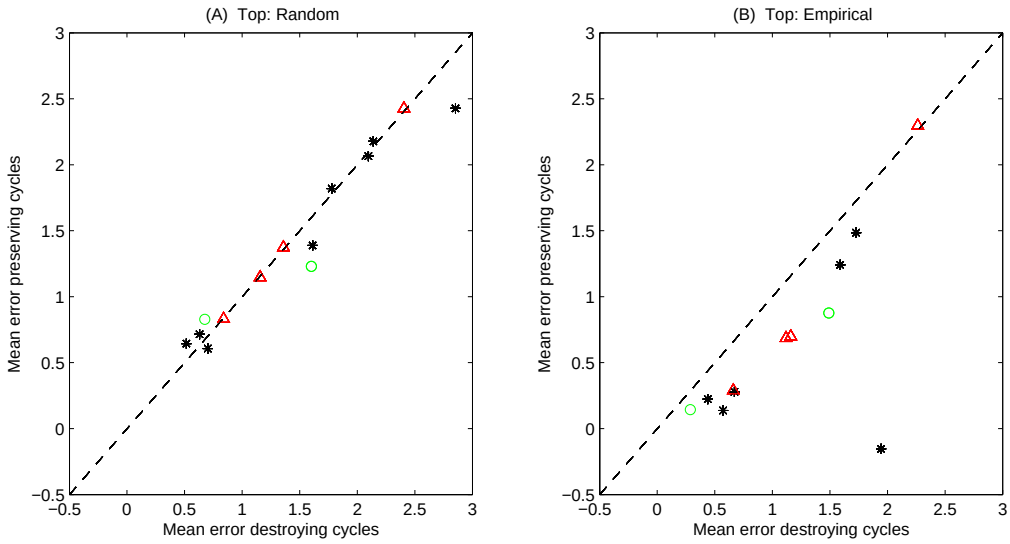

Figure 4: **Stability is enhanced by the position of cycles within the overall network topology.** The mean error $= \log_{10}(l_{\text{rand}}/l_{\text{emp}})$ of randomization algorithms that preserve cycles of length three plotted against the mean error of corresponding algorithms that change the same number of network links but do not preserve cycles. Randomizations in A and B destroy and preserve the original network topology respectively. See Appendix B for details of the randomization algorithms. Symbols indicate the method used to construct the community matrix: biomass flux = black stars (successional webs) or red triangles (soil webs); PPMR = green circles. Community matrices for which $< 90\%$ of randomizations produce distinct matrices are not shown; this includes all the EwE webs.

4 Random matrices and dynamic models

The results in Sec. 3 use the properties of general community matrices to indicate how stability may arise in complex networks. However, to truly understand the ecological implications of the results for random matrix models, it is helpful to consider a specific dynamic model rather than just a community matrix linearised around a hypothetical equilibrium point.

Most random matrix models, including those considered in Sec. 3, assume that all diagonal elements of the community matrix are the same, i.e. $a_{ii} = -d$ for some $d > 0$. This was justified by May (1972) with the statement "to set a time-scale, these damping times are all chosen to be unity" (i.e. $d = 1$). However, introducing the variability into the diagonal elements without changing their mean tends to increase the leading eigenvalue and this effect cannot be removed by a rescaling of variables (Haydon, 1994). Furthermore, the correspondence of diagonal elements with intraspecific effects is particular to simple generalised Lotka–Volterra models. More general models, for example with type-II functional responses or other nonlinear interaction terms, do not have this property and generate diagonal elements that depend on interspecific interactions (De Angelis, 1975; Haydon, 1994). Therefore, some variation in the diagonal elements of the community matrix should be expected. The assumption of identical diagonal elements is crucial yet ecologically unjustified. In this section, we show that a dynamic model that is constrained to have equal diagonal elements in the community matrix behaves fundamentally differently from an unconstrained model and cannot exhibit one of the most common mechanisms for species loss.

Although the results of May (1972) did not rely on a specific dynamic model, the simplest model that generates a community matrix of the type considered by May (1972) and

Allesina and Tang (2012) is a generalised Lotka–Volterra model

$$\frac{dx_i}{dt} = x_i \left(r_i + \sum_{j=1}^{S} q_{ij} x_j \right), \tag{5}$$

where x_i is the biomass density of species i, r_i is its intrinsic growth rate and the q_{ij} are referred to as Lotka–Volterra coefficients. This model assumes species interactions can be described by "mass action" (type-I) terms. The coefficients q_{ij} correspond to the dynamic index measure of interaction strength *sensu* Berlow et al. (1999) and can be estimated empirically from predator–prey mesocosms (Emmerson and Raffaelli, 2004). The diagonal element q_{ii} represents the strength of intraspecific competition, or self-limitation, for species i and must be non-positive to prevent boundless growth of species i in isolation. Although Eq. (5) is the simplest model of an ecological network, the conclusions of this section extend to more general models (see Appendix C).

The community matrix for Eq. (5) has elements $a_{ij} = q_{ij} x_i^*$. This helps to explain the row weight patterns seen in the empirically derived matrices in Sec. 3: the elements in row i of the community matrix are proportional to the equilibrium biomass density x_i^* of species i. This emphasises that the community matrix element a_{ij} does *not* represent the direct effect of species j on species i (which is q_{ij}) and a_{ii} does *not* represent the strength of intraspecific competition (which is q_{ii}).

The system in Eq. (5) undergoes a transcritical bifurcation whenever one of the equilibrium abundances x_i^* becomes negative. During this transition, the abundance of species i gradually declines to zero and the community moves smoothly to a different equilibrium, in which species i is absent. Instability and species loss are thus associated with the gradual decline of one species to zero density.

At a transcritical bifurcation, the equilibrium abundance x_i^* for species i is zero, and so the diagonal element of the community matrix for species i, $a_{ii} = q_{ii} x_i^*$, is also zero. Requiring all the diagonal elements of the community matrix to equal $-d < 0$ prevents

this type of transition from occurring. It also imposes a constraint on the intrinsic growth rates r_i (see Appendix C):

$$r_i = d \sum_{j=1}^{S} \frac{q_{ij}}{q_{jj}}. \tag{6}$$

This constraint means that the equilibrium biomasses are $x_i^* = -d/q_{ii}$, which are always all positive since $d > 0$ and $q_{ii} < 0$. Therefore, the only way in which a species can go extinct is via a degenerate bifurcation that makes the positive equilibrium become unstable, causing the system to move suddenly to a different equilibrium point (see Appendix C). Although sudden changes in community composition, such as regime shifts (Moellmann and Diekmann, 2012), are certainly possible, a model that precludes species loss via gradual decline is unable to capture one of the simplest and most common mechanisms for change in ecological communities (Rossberg, 2013). Hopf bifurcations, which lead to oscillatory dynamics, are also possible, but are not directly associated with species loss.

Eq. (6) can be interpreted as representing an ecological trade-off. A species that receives a net benefit from interactions with other species must compensate by having a negative intrinsic growth rate. For example, a top predator benefits from consuming prey ($q_{ij} \geq 0$), but will die out in the absence of prey ($r_i < 0$). Conversely, a species that is negatively impacted from interactions with other species (for example a basal resource, or a species that competes with other species) must compensate by having a positive intrinsic growth rate. Although the idea that such trade-offs may operate in specific ecological circumstances is easy to argue, it is implausible that the intrinsic growth rates will be precisely tuned to satisfy Eq. (6). Any slight deviation from Eq. (6) results in a shift in model behaviour, meaning that the assumption of equal diagonal elements makes the model structurally unstable.

Allesina and Tang (2012) argued that, in the limit as $S \to \infty$, variation among diagonal elements has a negligible effect on the leading eigenvalue compared to the effect of the off-diagonal elements. However, d_0 scales as $\sqrt{S}$. When scaling diagonal elements as $\sqrt{S}$

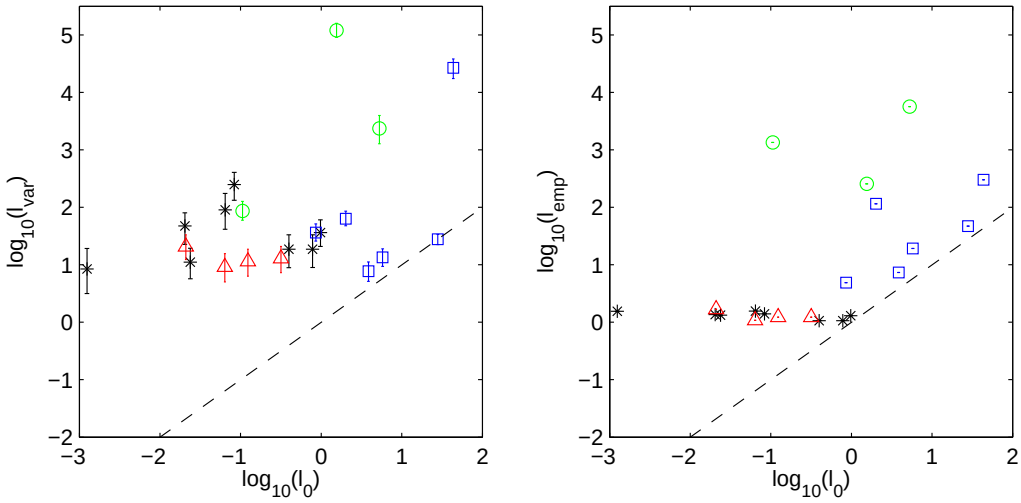

Figure 5: **Adding variability to the diagonals of empirically derived community matrices decreases stability by orders of magnitude.** The real part of the leading eigenvalue, l_0, of the matrix with diagonal elements set to zero against: (a) l_{var} the real part of the leading eigenvalue of the matrix with randomly generated diagonal elements with the same variance as the off-diagonals; (b) l_{emp} the real part of the leading eigenvalue of the matrix with empirically derived estimates for the diagonal elements. For each matrix with variable diagonal elements, a constant was added to all the diagonal elements so that their sum was zero. Symbols indicate the method used to construct the community matrix: biomass flux = black stars (successional webs) or red triangles (soil webs); EwE = blue squares; PPMR = green circles.

394 and keeping the coefficient of variation of the diagonal elements fixed, diagonal variance increases with network size. As a result, diagonal variance is not necessarily negligible
396 for stability considerations, even as $S \to \infty$. To quantify the effect of variability in the diagonal elements of the 21 empirically derived community matrices, we added variability
398 in one of two ways: firstly using randomly generated diagonal elements with the same variance as the off-diagonal elements, and secondly using the diagonal elements estimated
400 from the empirical food web data. To enable a meaningful quantitative comparison with the zero-diagonal case, the diagonal elements were shifted so that their mean was zero.

402 We compared the real part of the leading eigenvalue of the matrix with diagonal variability to that of the matrix with diagonal elements set to zero (l_0) (Fig. 5). For all 21 food
404 webs, using randomly generated diagonal elements (Fig. 5A) gives a leading eigenvalue with substantially larger real part than using equal diagonal elements. Using the empiri-
406 cally derived diagonal elements also gives a leading eigenvalue with larger real part in the majority of food webs (Fig. 5B). For one of the three community matrix construction
408 methods (that used for the soil food webs; black/red), the empirically derived diagonal elements dominate the matrix so strongly that all the matrices have approximately
410 the same leading eigenvalue when they are included. This shows that the standard assumption of equal diagonal elements consistently gives predictions that overestimate the
412 stability of the equilibrium.

5 Discussion

414 In the absence of detailed ecological data on species interactions, the use of random matrix models to make predictions about the relationship between ecosystem complexity
416 and stability is widespread (Thébault and Fontaine, 2010; Gravel et al., 2011; Allesina and Tang, 2012). We have shown that using randomly generated network topology and
418 interaction strengths can lead to predictions about local stability that differ by orders of

magnitude from those of empirically derived models.

Various characteristics of real food webs, for example the sign structure associated with predator–prey interactions (Allesina and Pascual, 2008; Jacquet et al., 2013), the network topology (Haydon, 2000; Tylianakis et al., 2010), the distribution (McCann et al., 1998; Emmerson and Raffaelli, 2004; Jacquet et al., 2013) and the relative positioning (Yodzis, 1981; De Ruiter et al., 1995; Neutel et al., 2002) of interaction strengths, have been suggested to have stabilising influences. Our results show that including such characteristics in models can increase stability but, even for larger networks where one would expect predictions based on random matrices to give the best results, this is not always the case.

Measuring species interaction coefficients directly in complex food webs is impossible. The models themselves are necessarily simplifications of the real ecology, ignoring, for example, details of age- and size-structure. They may also amalgamate species into perceived functional groups, which reduces the apparent species richness. Further assumptions and simplifications are necessary to convert empirical data into estimated community matrices. One of the strengths of our study is that the empirical matrices originate from three independently established sets of modelling assumptions: biomass flux model (Moore et al., 1996), Ecopath with Ecosim (Christensen and Pauly, 1992) and the predator–prey mass ratio model (Emmerson and Raffaelli, 2004). None of these approaches is "correct" and each has arisen from ecological and data-driven constraints specific to the systems under study. Nevertheless, the resulting community matrices represent our best estimates of ecological reality. Where consistent patterns emerge from our analysis of empirical networks derived in different ways, this provides evidence that these ecosystems contain structure that is not captured by simple random matrix models.

Our study shows that network topology may be less important for community stability than widely thought. For example, Tylianakis et al. (2010) summarised the attributes of network topology thought to confer stability. Our results in Fig. 3C, F, G show that it is possible to have two networks with identical topology but with key properties that

vary by up to four orders of magnitude. Conversely, our results in Fig. 3D show that a random network topology, with a particular organisation of interaction strengths, can come closer to empirical data. These results do not imply that topology has no effect, but they do show that it is less important than the distribution of interaction strengths.

We designed new randomization methods to quantify the role of two important features of real ecological networks, namely cycles of length three and row structure in the community matrix, in determining stability. We have shown that randomizations that preserve either of these properties better reflect the stability of the empirically derived network, although for cycles of length three the results are less marked than for row structure. That each of these properties involves a combination of network topology and the sizes of the community matrix elements emphasises our finding that results based on randomizations which ignore, or make unjustified assumptions about, either of these features do not usefully reflect ecological reality.

Previous studies have focused on different properties of community matrices. Neutel et al. (2007) saw a correlation between cycle weights and stability in data from soil food webs; Jacquet et al. (2013) found that removing trophic structure in community matrices from EwE models adversely affected stability; Tang et al. (2014) highlighted the role of pairwise correlation in community matrices constructed using allometric scaling laws based on body mass (Brose et al., 2006; Reuman et al., 2009; Pawar et al., 2012). Our study unifies these seemingly disparate findings by including community matrices constructed using each of these three methods and showing that different factors are more important for stability in these different types of community. For instance, pairwise correlation is important in communities where it is strong, but other factors, most notably row structure, dominate in communities where it is weaker.

Based on empirical and theoretical considerations, Rossberg (2013) argued that transcritical bifurcations, involving gradual decline of a species to zero density, are the dominant form of loss of local stability in ecological communities. Community matrices where the

diagonal elements are assumed to be equal prevent this type of change from happening and cannot, therefore, characterize the main type of instability that leads to change in community structure. The assumption of May (1972), that variations in the strength of intraspecific competition are unimportant, is one that has been largely neglected (see however De Angelis, 1975; Haydon, 1994; De Ruiter et al., 1995; Haydon, 2000; Neutel et al., 2002). The effect of this assumption is at least as prominent as the assumptions concerning off-diagonal community elements.

Technical detail and exhaustive testing are unavoidable ingredients in the preceding analysis, but a clear and practical biological message emerges. Although there is a relationship between "stability" and "complexity" in ecological communities, the predictive power of this relationship is weak. Honest and seemingly pragmatic attempts to replace ignorance of ecological detail with random numbers, whether these relate to network structure or to interactions between species, must be treated with extreme caution. Despite the limitations explained here in the context of local stability, random matrix models may be useful in the context of more general co-existence conditions, where they can lead to quantitative predictions of community structure in good agreement with observations (Meszéna et al., 2006; Rossberg, 2013).

On a further constructive note, we argue that using explicit dynamic models to describe ecological networks is preferable to directly assigning elements to a community matrix without reference to the underlying population dynamics. Parameterising a dynamic model requires additional data, for example species' intrinsic growth rates or equilibrium biomass densities, as well as estimates of interaction strengths. Collecting these data is not always practical. Nevertheless, estimating them via established models (De Ruiter et al., 1995; Emmerson and Raffaelli, 2004; Datta et al., 2010), or investigating the effects of introducing variability in them, is preferable to simply assuming that they satisfy an arbitrary set of mathematical constraints.

Acknowledgements

We thank Chris Hughes and Leonid Pastur for mathematical context and precision, Sarah Collings, Richard Law and Anje-Margriet Neutel for discussions and comments, Stefano Allesina for critical input and for sharing pre-prints of his publication with us, and Sebastian Diehl for insightful reviews. A.G.R. and J.B. were supported by the U.K. Department of Environment, Food and Rural Affairs (M1228), and the European Commission (agreement no. 308392, DEVOTES).

Online Appendices

A Empirically derived community matrices

The 21 empirically derived community matrices are available in electronic form. This section describes the methods used to obtain these data for each class of food web studied.

Biomass flux method

Eight successional soil food webs and four soil food webs were supplied by Anje-Margriet Neutel from the data published in De Ruiter et al. (1993); Moore et al. (1993); De Ruiter et al. (1995); Moore et al. (1996); Neutel et al. (2002). The elements of the community matrix were derived from a generalised Lotka–Volterra type model of the same form as Eq. (5) at equilibrium. For primary producers, $r_i > 0$ was the intrinsic rate of increase per year. For consumers, $r_i < 0$ was the non-predatory death rate per year. For a species i that is consumed by species j, the Lotka–Volterra coefficient q_{ij} was set equal to the negative of the consumption coefficient (in units of $\mathrm{g}^{-1}\ \mathrm{m}^2\ \mathrm{yr}^{-1}$) c_{ij}; the Lotka–Volterra coefficient q_{ji} was set equal to the assimilation efficiency of species j times the production efficiency of species j times the consumption coefficient c_{ij}. Species were aggregated into functional groups of species with similar food sources. Intrinsic birth and death rates and efficiencies were estimated from microcosm studies. Trophic interactions among taxa were established by direct observation or gut content analysis (Moore et al., 1996). Consumption coefficients were estimated from the measured biomass flux from prey to predator (Moore et al., 1993). The original data included a row and a column corresponding to detritus; these were removed for this analysis.

In the eight successional food webs, the average number of species in the webs was 12 (range 7–15), mean connectance was 0.29 (range 0.28 to 0.34) and average pairwise

correlation ρ (i.e. correlation between a_{ij} and a_{ji}) was -0.062 (range -0.02 to -0.13). In the four soil food webs, the average number of species in these webs was 17 (range 16–18), mean connectance was 0.27 (range 0.23 to 0.31) and average pairwise correlation ρ was -0.055 (range -0.047 to -0.059). All the networks were strictly predator–prey (i.e. a_{ij} and a_{ji} either had opposite signs or were both zero).

Predator–prey mass ratio method

Data were obtained for the average adult body mass w_i of species i and which species predated on which other species for the well documented Ythan Estuary (Emmerson and Raffaelli, 2004), Broadstone Stream (Woodward et al., 2005*b*) and Tuesday Lake 1984 (Jonsson et al., 2005) food webs. In the case of Tuesday Lake, 56 species were aggregated into 21 functional groups with identical links (trophic species). We used the average body mass of all species in a functional group as the body mass for that trophic species. Species with no observed predator or prey links were discarded.

The model of Emmerson and Raffaelli (2004) was used to estimate elements of the community matrix for both these food webs. For each predator–prey pair, the Lotka–Volterra coefficient q_{ij} was assumed to be a power-law function of the ratio of predator body size w_j to prey body size w_i:

$$q_{ij} = -q_0 \left(\frac{w_j}{w_i} \right)^{q_1}. \tag{A.1}$$

The corresponding element q_{ji} is opposite in sign and reduced in magnitude by a factor ϵ_j representing the predator's feeding efficiency: $q_{ji} = -\epsilon_j q_{ij}$. The equilibrium biomass x_i^* of species i was estimated to be

$$x_i^* = x_0 w_i^{q_2}, \tag{A.2}$$

The community matrix elements were then calculated via $a_{ij} = q_{ij} x_i^*$. Parameter values: $q_0 = 7 \times 10^{-4}$, $x_0 = 95.92$, $q_1 = 0.66$, $q_2 = -0.1836$. A fixed efficiency of $\epsilon = 0.1$ was used

for all species.

The average number of species in these webs was 47 (range 21–88), mean connectance was 0.24 (range 0.11 to 0.32) and average pairwise correlation ρ was -0.75 (range -0.28 to -0.98).

Ecopath with Ecosim

The Ecosim community matrices were constructed in two steps. First, an Ecopath (Christensen and Pauly, 1992) model was set up, representing a balanced account of biomass flows through the ecosystem, constrained by empirical data on abundances, metabolic rates and feeding preferences. From such a static Ecopath model, a dynamic Ecosim model was derived by modelling energy flows as outcomes of population-dynamic processes (feeding, respiration, mortality). This led to expressions for $\mathbf{f}(\mathbf{x})$, from which the community matrix can be computed. The time derivatives $\mathbf{f}(\mathbf{x})$ were given by the derivt function of Ecosim. Numerically differentiating the output of this function with respect to the biomass x_j of species j gives the j^{th} column of the community matrix.

The six marine food webs were: (i) the Tampa Bay model, which is a subset consisting of 52 groups of the Gulf of Mexico model (Walters et al., 2006), (ii) the Georgia Strait (British Columbia) model (Dalsgaard et al., 1998), a model consisting of 27 functional groups, (iii) the Caribbean reef model (50 groups Opitz, 1996),(iv) the North East Pacific model (40 groups Guénette and Christensen, 2005), (v) the Great Barrier Reef model (32 groups Gribble, 2005) and (vi) the Cefas North Sea model (70 groups Mackinson and Daskalov, 2007). The Ecopath with Ecosim (EwE) models for datasets (i)–(v) can be downloaded from the University of British Columbia website (sources.ecopath.org – password required for (i) and (ii) and may be found at www.ecopath.org/models for (iii)–(v)). The model for dataset (vi) is available by contacting one of the Cefas authors.

All of these food webs contain a substantial number of non-predator–prey interactions,

where either a_{ij} and a_{ji} have the same sign, or one of a_{ij} and a_{ji} is zero and the other is non-zero. The Tampa Bay and North Sea models contain multi-stanza (i.e. age-structured) groups for the same species. Each stanza is a separate node and a part of the population of stanza m of species n flows into stanza $m+1$ of species n, creating a $(+,0)$ type link. Thus, it is not possible to order the species so that all elements in the lower matrix triangle are positive and all elements in the upper matrix triangle are negative. We therefore designed the randomization algorithms (see below) so that they can be applied to any community matrix, regardless of sign structure.

The average number of species in these webs was 45 (range 27–70), mean connectance was 0.56 (range 0.34 to 0.70) and average pairwise correlation ρ was -0.057 (range -0.0097 to -0.28).

Stability criteria

The values of d_0 in the stability criteria of Eq. (3) and Eq. (4) were calculated for each empirically derived community matrix. In these equations: S is the number of species in the matrix; C is the connectance (i.e. the number of links divided by $S(S-1)$); σ is the standard deviation of the non-zero off-diagonal matrix elements; E and V are the mean and variance respectively of all off-diagonal elements; ρ is the pairwise correlation (Tang et al., 2014)

$$\rho = \frac{\mathrm{E}(a_{ij}a_{ji}) - E^2}{V}. \tag{A.3}$$

The stability criterion in Eq. (3) is only valid for matrices where $\sqrt{SV}(1+\rho) > SE$ (Tang et al., 2014). This was checked and found to be true for all our empirically derived community matrices.

B Randomization algorithms

These algorithms randomize an $S \times S$ matrix $A = [a_{ij}]$ to create an $S \times S$ matrix $B = [b_{ij}]$. N_l is the number of non-zero off-diagonal elements and $C = N_l/(S(S-1))$ is the fraction of off-diagonal elements that are non-zero. The mean and standard deviation of the non-zero elements are μ and σ respectively. The mean of the positive and negative elements are μ_+, μ_-. The number of elements involved in a cycle of length three is N_c (in cases where links are not bidirectional, i.e. only one of a_{ij}, a_{ji} is non-zero, an element is considered to be in a cycle regardless of the signs of the element); the number of non-zero elements not involved in a cycle of length three is $N_0 = N_l - N_c$.

Off-diagonal algorithms

All the off-diagonal algorithms hold the diagonal elements zero. Any randomization that resulted in a species having no interactions (i.e. every entry in a row or column was zero) or contained no cycles was rejected as these randomizations have a zero leading eigenvalue. Algorithms used in Fig. 2 and 3 are:

A: Random topology; randomly generated entries. Each randomization has N_l entries sampled from a normal distribution $N(0, \sigma^2)$. Entries are positioned randomly.

B: Random topology with sign structure; randomly generated entries. Each randomization has N_l randomly positioned entries. Positive (negative) entries are sampled from the half-normal distribution with mean μ_+ (μ_-). For every element pair (a_{ij}, a_{ji}) (with $i < j$) in the empirically derived matrix with a particular sign structure, i.e. $(+,+)$, $(+,-)$, $(-,0)$, etc, there is a random pair (b_{kl}, b_{lk}) (with $k < l$) with the same sign structure.

C: Empirical topology; randomly generated entries. An element b_{ij} is non-zero if and only if the corresponding element in the empirically derived matrix, a_{ij} is non-zero.

Furthermore $\text{sign}(a_{ij}) = \text{sign}(b_{ij})$. Positive (negative) entries are sampled from the half-normal distribution with mean μ_+ (μ_-).

D: Random topology; randomly generated entries preserving row structure. Each randomization has N_l entries placed at random. The randomized matrix contains the same proportion of each pair type [$(+,+)$, $(-,0)$, $(+,-)$, etc.] as the original matrix. The mean of the positive [negative] entries of row i of the empirically derived matrix is μ_{i+} [μ_{i-}]. Where there are no entries of that sign in a row, the value of $\mu_{i\pm}$ from a populated row (chosen at random) is used instead. Positive [negative] entries in row i of the randomized matrix are sampled from a normal distribution with mean μ_{i+} [μ_{i-}] and CV 0.2.

E: Random topology; empirical entries (paired). Each element a_{ij}, where $i < j$, is moved to element b_{kl}, where $k < l$. For every move of a_{ij} to b_{kl} there is a corresponding move of a_{ji} to b_{lk} preserving the pair structure of the empirically derived matrix.

F: Empirical topology; empirical entries (paired). Each element pair (a_{ij}, a_{ji}), where $i < j$, is swapped with an element pair (a_{kl}, a_{lk}), where $k < l$, which has the same sign structure, i.e. $(+,+)$, $(-,+)$, $(0,-)$, etc.

G: Empirical topology; empirical entries (not paired). Every positive element is swapped with another positive element. Every negative element is swapped with another negative element.

H: Random topology; empirical entries (constrained within rows/columns). This algorithm permutes elements of the empirically derived matrix within rows, while preserving (a_{ij}, a_{ji}) pairs. Most of the empirically derived community matrices are organised with top predators in the upper rows and basal resources in the lower rows. This tends to lead a triangular structure in the matrix, where the lower-left triangle contains predominantly negative elements and upper-right triangle contains predominantly positive elements. This means that the lower triangle typically

contains elements that have, on average, larger magnitude than the elements in the upper triangle. The row structure of the empirically derived matrices therefore tends to be stronger in the lower triangle, so we designed the algorithm described above to preserve row structure in the lower triangle (and therefore column structure in the upper triangle).

Each non-zero lower triangle element a_{ij} (where $i > j$) is moved within the same row to b_{ik} (where $i > k$). To preserve the pair structure of the original matrix, this move of a_{ij} to a_{ik} is accompanied by a corresponding move of a_{ji} to b_{ki}.

We also tested a similar algorithm that preserved row structure in the upper triangle and column structure in lower triangle; this produced matrices with leading eigenvalues further away from the leading eigenvalue of the empirically derived matrix.

The randomization algorithms for Fig. 4 are:

A (vertical axis): Random topology holding cycles of length three; empirical entries (paired). This is a constrained version of randomization D from Fig. 2 and 3. The N_c elements that are part of a cycle of length three are fixed (i.e. their position was not changed). The remaining N_0 elements are moved as described in D above.

A (horizontal axis): Random topology holding some entries; empirical entries (paired). This is a constrained version of randomization D from Fig. 2 and 3. N_c elements are chosen at random. These elements are fixed. The remaining N_0 elements are moved as described in D above.

B (vertical axis): Empirical topology holding cycles of length three; empirical entries (paired). This is a constrained version of randomization E from Fig. 2 and 3. The N_c elements that are part of a cycles of length three are fixed. The remaining N_0 elements are swapped as described in E above.

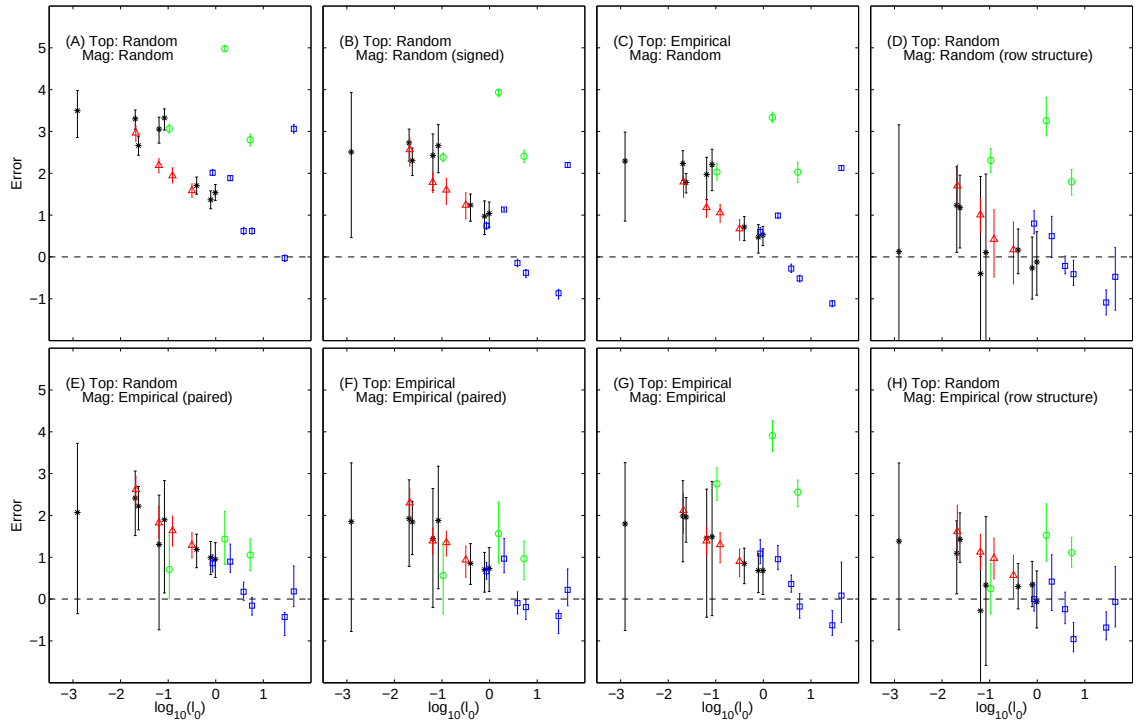

Supplementary Figure S1. Figure 3 redrawn with the matrices ordered by l_0, the real part of the leading eigenvalue of the empirically derived matrix, for the same six randomization algorithms (A–F) as in Fig. 3, changing either or both of network topology (Top) and magnitude of interaction strengths (Mag). Symbols indicate the method used to construct the community matrix: biomass flux = black stars (successional webs) or red triangles (soil webs); EwE = blue squares; PPMR = green circles.

B (horizontal axis): Empirical topology holding some entries; empirical entries (paired). This is a constrained version of randomization E from Fig. 2 and 3. N_c elements are chosen at random. These elements are fixed. The remaining N_0 elements are swapped as described in E above.

Supplementary Table S1 gives a summary of the properties preserved by each algorithm and measures of the bias in d.

Diagonal algorithm

In Fig. 5A, the diagonal elements were replaced with normally distributed random numbers with mean zero and variance σ^2, i.e. the variance of the non-zero off-diagonal

Figure	Pairs	Elements	Topology	Cycles	Rows	Limited changes	E(error)	P(under)
2A	×	×	×	×	×	×	2.29	0.03
2B	✓	×	×	×	×	×	1.7	0.14
2C	✓	×	✓	×	×	×	1.24	0.14
2D	×	×	×	×	✓	×	0.24*	0.42*
2E	✓	✓	×	×	×	×	1.21	0.13
2F	✓	✓	✓	×	×	×	1.01	0.16
2G	✓	✓	×	×	×	×	1.31	0.12
2H	✓	✓	×	×	✓	×	0.49	0.29
4A (y)	✓	✓	×	✓	×	✓	0.70	0.09
4A (x)	✓	✓	×	×	×	✓	0.77	0.05
4B (y)	✓	✓	✓	✓	×	✓	0.24	0.21
4B (x)	✓	✓	✓	×	×	✓	0.67	0.08

Supplementary Table S1. The properties preserved by each off-diagonal randomization algorithm. *Pairs:* $b_{ij} \neq 0$ if and only if $b_{ji} \neq 0$. *Elements:* the elements of the original matrix were permuted rather using than random deviates from a probability distribution. *Topology:* the original network topology was preserved. *Cycles:* the positions and weights of the cycles of length three was preserved. *Rows:* row structure was preserved. *Limited changes:* The number of elements of the original matrix that were moved was limited to be the same as in the corresponding cycle-preserving algorithm. E(error) is the mean value of error = $\log_{10}(l_{\text{rand}}/l_{\text{emp}})$ of 200 realisations of the randomization scheme across the 21 empirically derived matrices. P(under) is the proportion of realisations for which the error is negative. An unbiased randomization scheme would have E(error) = 0 and $mathrmP$(under) = 0.5. Entries marked * do not include the freshwater webs as this algorithm does not preserve pairwise structure and as expected gives very poor results for these matrices.

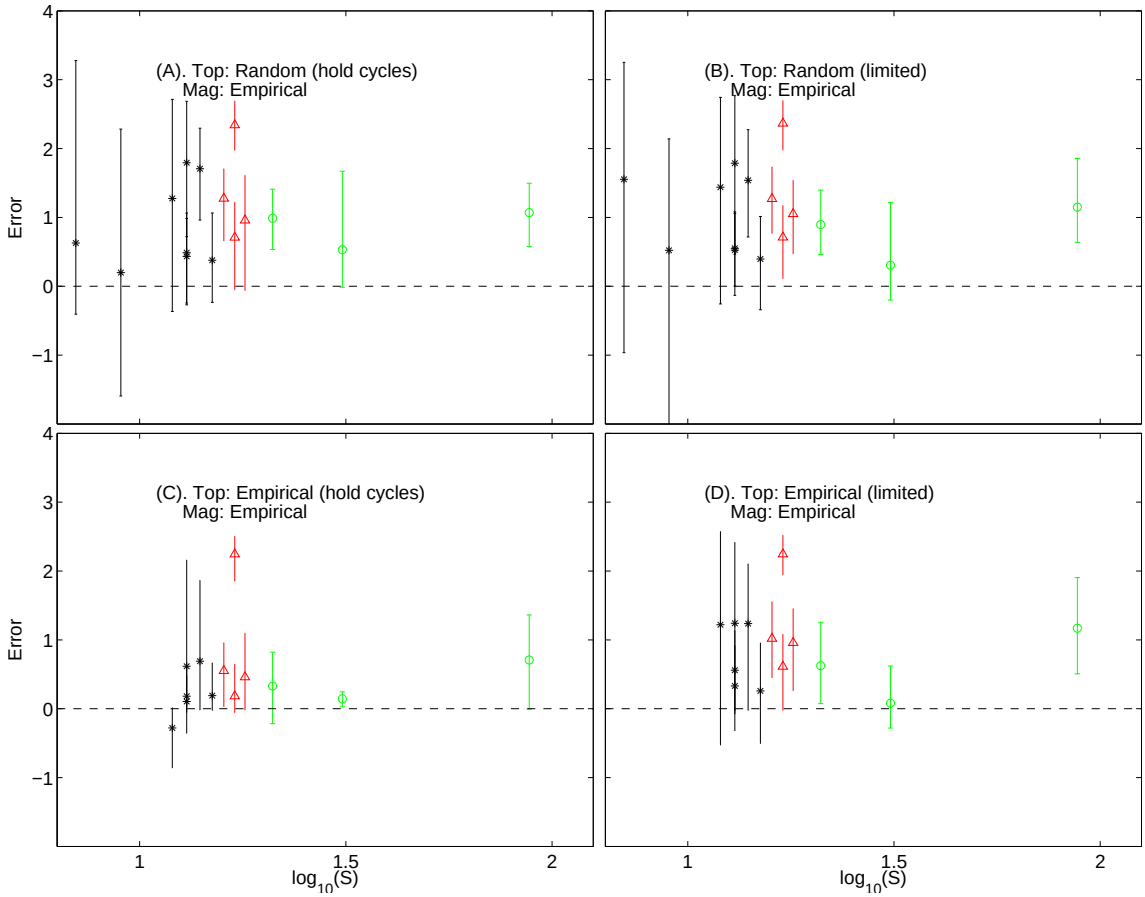

Supplementary Figure S2. The distribution of error = $\log_{10}(l_{\text{rand}}/l_{\text{emp}})$ for the four randomization algorithms used in Fig. 4. Fig. 4A plots algorithm A against algorithm B; Fig. 4B plots algorithm C against algorithm D. The food webs are plotted against the number of species S in the web on the horizontal axis. Symbols indicate the method used to construct the community matrix: biomass flux = black stars (successional webs) or red triangles (soil webs); PPMR = green circles. Community matrices for which $< 90\%$ of randomizations produce distinct matrices are not shown; this includes all the EwE webs.

elements.

C Dynamic model bifurcation analysis

Consider the generalised Lotka–Volterra model

$$\frac{dx_i}{dt} = x_i \left(r_i + \sum_{j=1}^{S} q_{ij} x_j \right), \qquad i = 1, \ldots, S, \tag{C.1}$$

where x_i is the biomass density of species i, r_i is the intrinsic growth rate of species i and the q_{ij} are Lotka–Volterra coefficients. To prevent boundless growth of species i in isolation, the elemnts q_{ii} must not be positive. Eq. (C.1) has an equilibrium point $\mathbf{x}^*$ satisfying $Q\mathbf{x}^* = -\mathbf{r}$. At this equilibrium, the diagonal elements of the community matrix are $a_{ii} = q_{ii}x_i^*$. If $x_i^* > 0$ for all i, this equilibrium corresponds to the coexistence of all species. If, as the model parameters are varied, x_j^* becomes negative for some j, there is a transcritical bifurcation and a different equilibrium, with $x_j^* = 0$, becomes stable. Hence, species j goes extinct via a gradual decline of x_j^* to zero and, at the transcritical bifurcation, $a_{jj} = 0$.

Now consider the effect of requiring the diagonal elements of the community matrix to be equal, $a_{ii} = -d < 0$. Combining this with the equilibrium condition $Q\mathbf{x}^* = -\mathbf{r}$ shows that the intrinsic growth rates r_i must satisfy

$$r_i = d \sum_{j=1}^{S} \frac{q_{ij}}{q_{jj}}, \qquad i = 1, \ldots, S, \tag{C.2}$$

which is Eq. (6) in the main text. This implies that basal species i, which are negatively influenced by their interactions with other species and so have $q_{ij} < 0$, will always have positive r_i (recall that $q_{jj} < 0$). Top predators, which are positively influenced by their interactions and so have $q_{ij} > 0$ $(i \neq j)$ will typically have negative r_i.

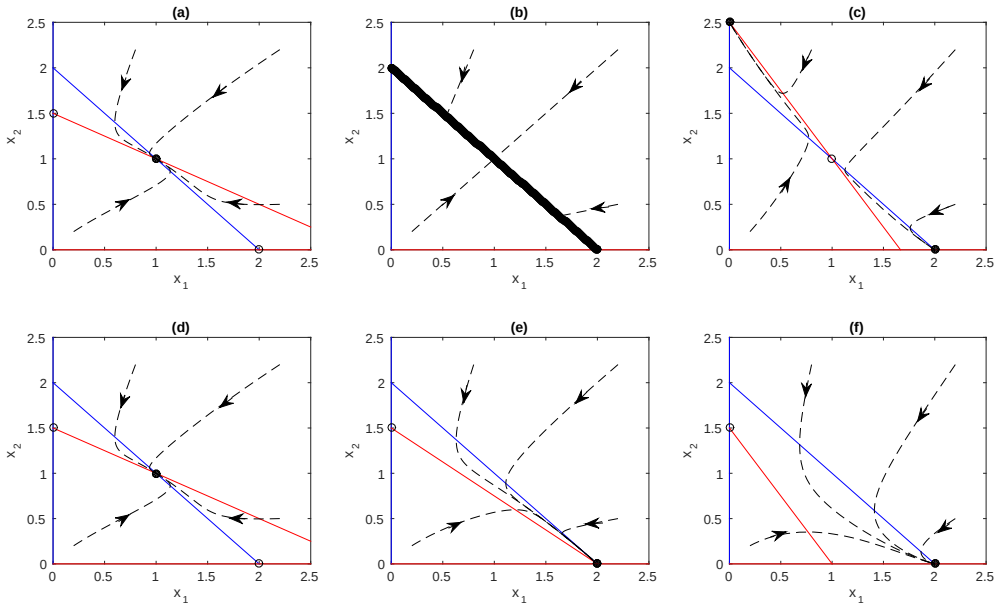

Supplementary Figure S3. Phase planes for a two-species generalised Lotka–Volterra model (C.1). The blue lines are x_1 nullclines, the red lines are x_2 nullclines, the circles are equilibria (filled = stable; open = unstable) and the dashed curves are example orbits. **(a–c)** Parameters are constrained by Eq. (C.2): the nullclines are forced to cross at $(x_1, x_2) = (-d/q_{11}, -d/q_{22})$, which is always in the interior of the positive quadrant; at the bifurcation (b), the nullclines lie on top of another creating a line of non-isolated equilibria; after the bifurcation (c), one of the two species suddenly goes extinct (which species goes extinct depends on the initial condition). **(d–f)** Parameters are not constrained: as the x_2 nullcline steepens, the equilibrium density of species 2 gradually declines until the equilibrium collides with the single-species equilibrium on the x_1 axis, at which point a transcritical bifurcation occurs (e); after the bifurcation (f), species 2 is extinct. Parameter values: $r_1 = 2$, $q_{11} = q_{22} = q_{12} = -1$; (a) $q_{21} = -0.5$, $r_2 = 1.5$; (b) $q_{21} = -1$, $r_2 = 2$; (c) $q_{21} = -1.5$, $r_2 = 2.5$; (d) $q_{21} = -0.5$, $r_2 = 1.5$; (e) $q_{21} = -0.75$, $r_2 = 1.5$; (f) $q_{21} = -1.5$, $r_2 = 1.5$.

Under the constraint in Eq. (C.2), the equilibrium equation $Q\mathbf{x}^* + \mathbf{r} = \mathbf{0}$ becomes $Q(\mathbf{x}^* - \mathbf{v}) = \mathbf{0}$, where $v_i = -d/q_{ii}$, which is always positive since $d > 0$ and $q_{ii} < 0$. Hence, there is always a positive equilibrium with $x_i^* = v_i$. This equilibrium cannot undergo a transcritical bifurcation with another equilibrium for which $v_j^* = 0$ for some j. The only way a species can go extinct is if the matrix Q becomes rank-deficient, which leads to a line of non-isolated equilibria through the point $\mathbf{x}^* = \mathbf{v}$. The positive equilibrium at $\mathbf{x}^* = \mathbf{v}$ suddenly becomes unstable and an equilibrium in which one or more species is zero suddenly becomes stable.

Supplementary Fig. S3 illustrates the bifurcation structure of the model, with and without the constraint imposed by Eq. (C.2), for the simple two-species case. In the constrained model (Fig. S3(a–c)), the two nullclines are forced to intersect at the point $(x_1, x_2) = (-d/q_{11}, -d/q_{22})$. As the q_{ij} are varied, the equilibrium must always remain in the interior of the positive quadrant, because q_{ii} must be non-positive and finite. Therefore, no transcritical bifurcations are possible. The only way in which a species can go extinct is if the nullclines become parallel (in the two-species model, this requires q_{12} and q_{21} have the same sign). If this happens, the nullclines coincide and there is a line of non-isolated equilibria passing through $(-d/q_{11}, -d/q_{22})$. After this bifurcation, the equilibrium at $(-d/q_{11}, -d/q_{22})$ loses stability and one of the two species goes extinct.

In the unconstrained model (Fig. S3(d–f)), the slopes and intercepts of the nullclines can vary independently as model parameters are varied. The coexistence equilibrium point can therefore move outside the positive quadrant and lose stability via a transcritical bifurcation. For example, in the transition from Supplementary Fig. S3(d) to S3(e), species 2 gradually declines to zero, at which point there is a transcritical bifurcation. The coexistence equilibrium moves outside the feasible region and the species 1 equilibrium $(x_1, x_2) = (0, -r_2/q_{22})$ becomes stable.

In Supplementary Fig. S3, we used a competition model ($q_{12}, q_{21} < 0$) because, in the constrained two-species case, a bifurcation can only occur model when $q_{12}q_{21} = 1$, which

requires q_{12} and q_{21} to have the same sign. For models with more species, the scenario is not limited to competitive interactions: bifurcations occur in the constrained model when the matrix Q becomes rank-deficient, which can happen in predator–prey models as well as competition models.

The result that constraining diagonal elements of the community matrix to be equal precludes transcritical bifurcations is not particular to the generalised Lotka–Volterra model in Eq. (C.1). Consider a more general model where the rate of change of species i is

$$\frac{dx_i}{dt} = x_i \left(r_i + q_{ii}x_i + h_i(\mathbf{x})\right), \qquad i = 1, \ldots, S, \tag{C.3}$$

for some function $h_i(\mathbf{x})$. If we require that $(x_j = 0\ \forall j \neq i\ \Rightarrow\ h_i(\mathbf{x}) = 0)$ then, as for the generalised Lotka–Volterra model, each species, in isolation, behaves according to a logistic equation with intrinsic growth rate r_i (which can be positive or negative) and carrying capacity $-r_i/q_{ii} > 0$. However, the generalised Lotka–Volterra model assumes that $h_i(\mathbf{x})$ is a linear function of the x_i, whereas in Eq. (C.3) the interaction terms contained in $h_i(\mathbf{x})$ can be nonlinear, for example representing a type-II response. The diagonal elements of the Jacobian matrix are

$$a_{ii} = r_i + 2q_{ii}x_i + h_i(\mathbf{x}) + x_i\frac{\partial h_i}{\partial x_i}. \tag{C.4}$$

Using the equilibrium condition from setting Eq. (C.3) equal to 0, we obtain the diagonal elements of the Jacobian matrix at equilibrium:

$$a_{ii} = x_i^* \left(q_{ii} + \left.\frac{\partial h_i}{\partial x_i}\right|_{\mathbf{x}=\mathbf{x}^*}\right). \tag{C.5}$$

This shows that, if species i goes extinct via a transcritical bifurcation ($x_i^* = 0$), then its diagonal element in the community matrix (a_{ii}) must also be zero at the bifurcation point. If instead the diagonal elements a_{ii} are all constrained to equal $-d$, then the equilibrium

satisfies

$$x_i^* = -\frac{d}{q_{ii} + \left.\frac{\partial h_i}{\partial x_i}\right|_{\mathbf{x}=\mathbf{x}^*}}. \tag{C.6}$$

Unlike in the constrained generalised Lotka–Volterra model, there is not always a unique positive equilibrium. There may be 0, 1 or more solutions to Eq. (C.6), some of which may have $x_i^* < 0$ for some species. There may be saddle-node bifurcations that change the number of equilibria and there may be Hopf bifurcations that change the stability of equilibria. Nevertheless, Eq. (C.6) shows that it is impossible for x_i^* to pass smoothly through 0 as a model parameter is varied. Hence, transcritical bifurcations are impossible.

In general, requiring the diagonal elements of the community matrix to be equal imposes S constraints (e.g. Eq. (C.2)) on the model parameters. This is equivalent to taking a codimension S slice through the full model parameter space. The full parameter space is dominated by transcritical bifurcations, whereas the constrained codimension S parameter space has no transcritical bifurcations. The constrained model is therefore a singular case. It does not give a representative picture of the ways in which equilibria can gain or lose stability.

References

762 Allesina, S., and M. Pascual. 2008. Network structure, predator–prey modules, and stability in large food webs. Theoretical Ecology 1:55–64.

764 Allesina, S., and S. Tang. 2012. Stability criteria for complex ecosystems. Nature 483:205–208.

766 Bastolla, U., M. A. Fortuna, A. Pascual-García, A. Ferrera, B. Luque, and J. Bascompte. 2009. The architecture of mutualistic networks minimizes competition and increases 768 biodiversity. Nature 458:1018–1020.

Berlow, E. L., S. A. Navarrete, C. J. Briggs, M. E. Power, and B. A. Menge. 1999. 770 Quantifying variation in the strengths of species interactions. Ecology 80:2206–2224.

Brose, U., R. J. Williams, and N. D. Martinez. 2006. Allometric scaling enhances stability 772 in complex food webs. Ecology Letters 9:1228–1236.

Christensen, V., and D. Pauly. 1992. ECOPATH II–a software for balancing steady-774 state ecosystem models and calculating network characteristics. Ecological modelling 61:169–185.

776 Dalsgaard, J., S. S. Wallace, S. Salas, and D. Preikshot. 1998. Mass-balance model reconstructions of the Strait of Georgia: the present, one hundred, and five hundred 778 years ago. Pages 72–91 *in* D. Pauly, T. Pitcher, D. Preikshot, and J. Hearne, eds. Back to the future: reconstructing the Strait of Georgia ecosystem. Vol. 6 of *Fisheries* 780 *Centre Research Reports*.

Dambacher, J. M., H.-K. Luh, H. W. Li, and P. A. Rossignol. 2003. Qualitative stability 782 and ambiguity in model ecosystems. The American Naturalist 161:876–888.

Datta, S., G. W. Delius, and R. Law. 2010. A jump-growth model for predator–prey 784 dynamics: derivation and application to marine ecosystems. Bulletin of mathematical biology 72:1361–1382.

De Angelis, D. L. 1975. Stability and connectance in food web models. Ecology 56:238–243.

De Ruiter, P. C., A.-M. Neutel, and J. C. Moore. 1995. Energetics, patterns of interaction strengths, and stability in real ecosystems. Science 269:1257–1257.

De Ruiter, P. C., J. A. Van Veen, J. C. Moore, L. Brussaard, and H. W. Hunt. 1993. Calculation of nitrogen mineralization in soil food webs. Plant and Soil 157:263–273.

Elton, C. S. 1958. The ecology of invasions by animals and plants. Methuen, London.

Emmerson, M. C., and D. Raffaelli. 2004. Predator–prey body size, interaction strength and the stability of a real food web. Journal of Animal Ecology 73:399–409.

Emmerson, M. C., and J. M. Yearsley. 2004. Weak interactions, omnivory and emergent food-web properties. Proceedings of the Royal Society of London. Series B: Biological Sciences 271:397–405.

Erdős, P., and A. Rényi. 1960. On the evolution of random graphs. Publ. Math. Inst. Hungar. Acad. Sci 5:17–61.

Gravel, D., E. Canard, F. Guichard, and N. Mouquet. 2011. Persistence increases with diversity and connectance in trophic metacommunities. PLoS One 6:e19374, DOI:10.1371/journal.pone.0019374.

Gribble, N. A. 2005. Ecosystem modelling of the great barrier reef: A balanced trophic biomass approach. Pages 2561–2567 *in* A. Zerger and R. M. Argent, eds. MODSIM 2005 International Congress on Modelling and Simulation.

Grimm, V., and C. Wissel. 1997. Babel, or the ecological stability discussions: an inventory and analysis of terminology and a guide for avoiding confusion. Oecologia 109:323–334.

Guénette, S., and V. Christensen. 2005. Food web models and data for studying fisheries and environmental impacts on eastern pacific ecosystems. Tech. Rep. 13(1), University of British Columbia.

Haydon, D. 1994. Pivotal assumptions determining the relationship between stability and complexity: an analytical synthesis of the stability-complexity debate. American Naturalist 144:14–29.

Haydon, D. T. 2000. Maximally stable model ecosystems can be highly connected. Ecology 81:2631–2636.

Hofbauer, J., and K. Sigmund. 1998. Evolutionary games and population dynamics. Cambridge University Press, Cambridge.

Jacquet, C., C. Moritz, L. Morissette, P. Legagneux, F. Massol, P. Archambault, and D. Gravel. 2013. No complexity-stability relationship in natural communities. arXiv preprint, arXiv:1307.5364 .

Jansen, W. 1987. A permanence theorem for replicator and lotka-volterra systems. Journal of Mathematical Biology 25:411–422.

Jonsson, T., J. E. Cohen, and S. R. Carpenter. 2005. Food webs, body size, and species abundance in ecological community description. Advances in ecological research 36:1–84.

Law, R., and J. C. Blackford. 1992. Self-assembling food webs: a global viewpoint of coexistence of species in lotka-volterra communities. Ecology 73:567–578.

Levins, R. 1979. Coexistence in a variable environment. American Naturalist 114:765–783.

MacArthur, R. 1955. Fluctuations of animal populations and a measure of community stability. ecology 36:533–536.

Mackinson, S., and G. Daskalov. 2007. An ecosystem model of the North Sea to support
834 an ecosystem approach to fisheries management: description and parameterisation. Cefas Science Series Technical Report 142:195.

836 May, R. M. 1972. Will a large complex system be stable. Nature 238:413–414.

McCann, K., A. Hastings, and G. R. Huxel. 1998. Weak trophic interactions and the
838 balance of nature. Nature 395:794–798.

McCann, K. S. 2000. The diversity–stability debate. Nature 405:228–233.

840 Meszéna, G., M. Gyllenberg, L. Pásztor, and J. A. J. Metz. 2006. Competitive exclusion and limiting similarity: a unified theory. Theoretical Population Biology 69:68–87.

842 Metha, M. L. 1967. Random matrices and the statistical theory of energy levels. Academic, New York .

844 Moellmann, C., and R. Diekmann. 2012. Marine ecosystem regime shifts induced by climate and overfishing: A review for the northern hemisphere. Advances in Ecological
846 Research 47:303–347.

Moore, J. C., P. C. De Ruiter, and H. W. Hunt. 1993. Influence of productivity on the
848 stability of real and model ecosystems. Science 261:906–908.

Moore, J. C., P. C. de Ruiter, H. W. Hunt, D. C. Coleman, and D. W. Freckman. 1996.
850 Microcosms and soil ecology: Critical linkages between fields studies and modelling food webs. Ecology 77:694–705.

852 Neutel, A.-M., J. A. P. Heesterbeek, and P. C. de Ruiter. 2002. Stability in real food webs: weak links in long loops. Science 296:1120–1123.

854 Neutel, A.-M., J. A. P. Heesterbeek, J. van de Koppel, G. Hoenderboom, A. Vos, C. Kaldeway, F. Berendse, and P. C. de Ruiter. 2007. Reconciling complexity with
856 stability in naturally assembling food webs. Nature 449:599–602.

O'Gorman, E. J., and M. C. Emmerson. 2010. Manipulating interaction strengths and the consequences for trivariate patterns in a marine food web. Advances in Ecological Research 42:301–419.

Opitz, S. 1996. Trophic interactions in caribbean coral reefs. Tech. Rep. 43, International Center for Living Aquatic Resources Management.

Otto, S. B., B. C. Rall, and U. Brose. 2007. Allometric degree distributions facilitate food-web stability. Nature 450:1226–1229.

Pawar, S., A. I. Dell, and V. M. Savage. 2012. Dimensionality of consumer search space drives trophic interaction strengths. Nature 486:485–489.

Pimm, S. L. 1980. Food web design and the effect of species deletion. Oikos 35:139–149.

Pimm, S. L., and J. H. Lawton. 1978. On feeding on more than one trophic level. Nature 275:542–544.

Reuman, D. C., C. Mulder, C. Banašek-Richter, M.-F. Cattin Blandenier, A. M. Breure, H. D. Hollander, J. M. Kneitel, D. Raffaelli, G. Woodward, and J. E. Cohen. 2009. Allometry of body size and abundance in 166 food webs. Advances in Ecological Research 41:1–44.

Rossberg, A. G. 2013. Food webs and biodiversity: foundations, models, data. Wiley.

Staniczenko, P. P. A., J. C. Kopp, and S. Allesina. 2013. The ghost of nestedness in ecological networks. Nature communications 4:1391.

Tang, S., S. Pawar, and S. Allesina. 2014. Correlation between interaction strengths drives stability in large ecological networks. Ecology Letters 17:1094–1100.

Thébault, E., and C. Fontaine. 2010. Stability of ecological communities and the architecture of mutualistic and trophic networks. Science 329:853–856.

880 Twomey, M., U. Jacob, and M. C. Emmerson. 2012. Perturbing a marine food web: Consequences for food web structure and trivariate patterns. Advances in Ecological 882 Research 47:349–409.

Tylianakis, J. M., E. Laliberté, A. Nielsen, and J. Bascompte. 2010. Conservation of 884 species interaction networks. Biological conservation 143:2270–2279.

Walters, C., S. J. D. Martell, and B. Mahmoudi. 2006. An Ecosim model for exploring 886 ecosystem management options for the Gulf of Mexico: implications of including multistanza life history models for policy predictions. Page 23 *in* Presentation for Mote 888 Symposium. Vol. 6.

Wiggins, S. 2003. Introduction to applied nonlinear dynamical systems and chaos, vol. 2. 890 Springer.

Woodward, G., B. Ebenman, M. Emmerson, J. M. Montoya, J. M. Olesen, A. Valido, and 892 P. H. Warren. 2005*a*. Body size in ecological networks. Trends in ecology & evolution 20:402–409.

894 Woodward, G., D. C. Speirs, and A. G. Hildrew. 2005*b*. Quantification and resolution of a complex, size-structured food web. Advances in ecological research 36:85–135.

896 Yodzis, P. 1981. The stability of real ecosystems. Nature 289:674–676.